Control of External Kink Modes Near the Ideal Wall Limit Using Kalman Filtering and Optimal Control Techniques

D. A. Maurer, J. Bialek, A. H. Boozer, B. DeBono, J. M. Hanson, R. James, J. P. Levesque, O. Katsuro-Hopkins, M. E. Mauel, G. A. Navratil, T. S. Pedersen, and D. Shiarki

Dept. of Applied Physics & Applied Mathematics, Columbia University, New York, USA

e-mail contact of main author: dam22@columbia.edu

Abstract. The first experimental demonstration of active feedback suppression of rotating external kink modes near the ideal wall limit in a tokamak using Kalman filtering to discriminate the $n = 1$ kink mode from background noise is presented [1]. The Kalman filter contains a model that captures the dynamics of a rotating, growing $n = 1$ kink mode. Suppression of the external kink mode is demonstrated using this Kalman filter over a broad range of phase angles between the sensed mode and applied control field, and performance is robust at noise levels that render simple proportional and derivative gain feedback ineffective. The demonstrated experimental utility of a such a Kalman filter in affecting the external kink motivates development of more complete physics model based filters and the incorporation of methods to optimize the control system gain used to stabilize the resistive wall kink mode. We also present new results that indicate that the use of such optimal control feedback with a model reduction based eigen-mode representation of a VALEN finite element model of resistive wall mode feedback leads to enhanced performance for the base-line ITER wall mode control system in comparison to traditional, classical control law based systems [2].

1 Introduction

We report on the first experimental demonstration of feedback suppression of rotating $m/n = 3/1$ external kink modes near the ideal wall limit in a tokamak using Kalman filtering to discriminate $n = 1$ kink mode amplitude from background magnetohydrodynamic and additive white noise [1]. Kalman filtering was observed to suppress the kink over a broad range of feedback phase angles between the sensed mode and applied control field. This suppression is accomplished with minimal excitation of higher frequencies under feedback as was observed in previous experiments using simple lead-lag loop compensation [3]. The importance of these results in relation to achieving the highest plasma pressure limits in ITER and other future fusion devices is clear [4]. The use of advanced control algorithms to stabilize the resistive wall kink beyond the use of Kalman filtering for mode measurements is a possible avenue to improve upon the experimental results presented here. A computational study of a novel resistive wall mode Kalman filter and feedback controller designed using model reduction and optimal control theory is presented for ITER that allows operation up to 86% of the ideal wall limit using the present design external control coils and employing only proportional gain [2]. We find an order of magnitude reduction of the required control coil current and voltage in the presence of white noise from the no-wall limit to the optimal feedback system performance limit as compared with a traditional, classical controller. Improved understanding and control of long-wavelength kink instabilities that grow on the resistive time scale of a nearby conducting wall, τ_w, is a key issue for tokamak-based fusion reactors. These resistive wall kink modes appear when opposing fields from eddy currents in the wall prevent growth of fast ideal modes. When the wall mode is controlled, tokamaks and spherical tori can operate steadily with high plasma pressure that exceeds the no-wall pressure limit. This makes possible advanced scenarios having good confinement and low current drive power requirements. The wall mode has been stabilized either by sustained plasma rotation [5, 6, 7] or by active feedback control [1, 8, 9, 10].

2   HBT-EP Kink Mode Control System

The HBT-EP experiment incorporates a segmented, close fitting wall made from alternating stainless steel and aluminum sections (see Fig. 1). The wall sections may be independently positioned in the minor radial direction between $r = 15$ cm and $r = 23$ cm. Each of the 10 toroidal locations has either a pair of stainless steel shells or a pair of aluminum shells. The aluminum shells are 1.4 cm thick and have an eddy current decay time of 60 msec. By contrast, the stainless steel shells have a thickness of 0.2 cm and an eddy current decay time of 300 μsec. In the presence of such a conducting wall, external kink instabilities that would otherwise grow on the Alfvenic time-scale τ_A grow instead

FIG. 1: HBT-EP plasma, conducting wall, and control system geometry showing location of magnetic sensors and control coils.

on the wall's eddy current decay time-scale τ_w. It is these slowly growing wall kink modes that are amenable to feedback control due to there reduced growth rates. HBT-EP's mode control feedback system employs an array of twenty poloidal magnetic pickup coils as sensors, and twenty pairs of radial magnetic coils serve as actuators. Both the sensor and control coils are well-coupled to the plasma, by virtue of being mounted on thin, stainless steel walls that can be positioned up to 1 cm from the plasma surface. Coupling between the sensor and control coils is minimal because nearby control-sensor pairs apply and detect mutually orthogonal magnetic fields. Figure 1 also shows the arrangement of control and sensor coils on the stainless steel shells.
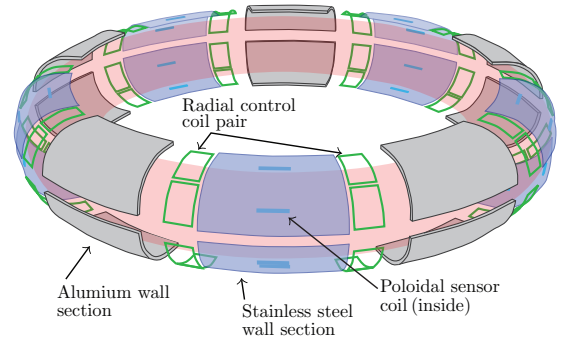
The control and sensor coils are divided into four independent feedback loops, each consisting of five sensor coils and control coil pairs driven by a field-programmable gate array (FPGA) controller. The coils in each feedback loop are spaced evenly in the toroidal direction at the same fixed poloidal angle. RC filtering is used to partially integrate the sensor coil signals and remove quasi-dc offsets before the signals are sent to the FPGA digital controller (see Fig. 2). Audio frequency range power amplifiers following the FPGA can drive a maximum of 5 Amperes at 5 kHz in each control coil pair. The FPGA controllers contain programmable arrays of semiconductor logic and memory blocks. They provide a platform for parallelized hardware implementation of control algorithms and are capable of operating at low latencies. The control algorithm presently in use executes with total latency of 12 μsec, with a sample rate of 5 μsec.

For previous feedback studies, an algorithm with spatial and temporal filtering was implemented on the FPGAs [3]. The spatial filter used a discrete Fourier transform (DFT) to separate a toroidal $n = 1$ mode from any $n = 0$ and $n = 2$ activity, and to apply a rotation operator that allowed for arbitrary adjustments in the spatial phasing of the feedback magnetic field. The temporal filter applied corrections to the open-loop hardware transfer function using a second order, phase lead-lag compensator. These filters are retained for present work, with
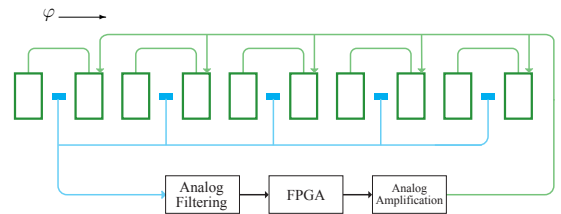

FIG. 2: Physical arrangement of one of four feedback control loops showing layout of the sensor coils (blue), control coil pairs (green), and analog and digital control circuitry.

the second order temporal filter broken into two first order filters of the form, $y_i = a_0 x_i + a_1 x_{i-1} + b_1 y_{i-1}$. Here, the filtered output y_i at time step i is given in terms of an input x_i and the value of the filter's input and output at the previous time step. The algorithm is augmented with a Kalman filter in order to discriminate the unstable plasma mode from background noise and other MHD activity.

Kalman filtering has several advantages over traditional frequency domain filtering. It is designed in the time domain, and a linear model of the system of interest is incorporated in to the filter. Physics models and measurement capabilities exist for many systems, but both the model and measurements may be limited in their ability to fully characterize the state of the system by noise or lack of completeness. The Kalman filter provides a way of comparing available measurements with the output of a model in real time to estimate the actual state of the system. The system states estimated for the HBT-EP Kalman filter are the cosine and sine components of the polodial magnetic field of a rotating, growing $n = 1$ kink mode. The system model used is that of a growing, rotating mode which advances the state of a mode rotating at a fixed angular rotation rate ω and growth rate γ [1]. The Kalman filter advances the model, adjusting its internal model for the amplitude and phase of the mode based on the measured inputs. This model is based upon a simplified limit of the more detailed physics description of rotating kink modes developed and used to understand MHD spectroscopy experiments on HBT-EP [11].

3   Kink Mode Kalman Filtering Experiments

In order to study the efficacy of Kalman filter feedback on external kink modes, current driven kinks were excited in HBT-EP by ramping the plasma current. When the current ramp is sufficiently steep, the current density profile becomes very broad with a large edge current density. Under these conditions, rotating external kink modes that are resonant with a rational q-surface just outside of the plasma are observed. The rotation rate of the modes is near 5 kHz, their growth rate is about 2–3 msec^{-1}, and they are believed to be near the ideal wall stability limit [11, 12]. Feedback with the Kalman filter algorithm was observed to both suppress and excite the magnetic fluctuations of the mode according to the spatial phasing $\Delta\Phi_f$ of the applied field relative to that of the mode. To produce the phase-frequency plot in Fig. 3, the feedback phase angle was scanned in 10° increments, and three discharges were made for each setting. Fluctuations measured by a poloidal sensor coil were then Fourier analyzed and averaged together by phase angle. The results show clear regions of excitation and suppression in the 5 kHz band, separated in $\Delta\Phi_f$-space by 180°. No significant excitation of frequencies above 8 kHz was observed at any setting of the feedback phase angle.
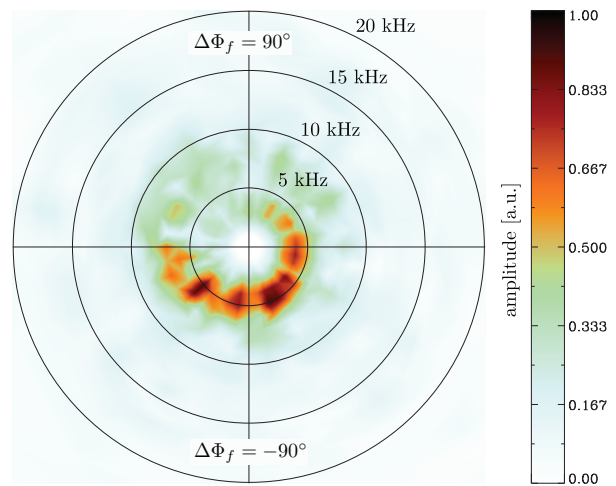

FIG. 3: Frequency spectrum of poloidal field fluctuations in arbitrary units as a function of the phase angle between feedback and the measured $n = 1$ mode. Feedback may be phased to either suppress or excite the mode near 5 kHz, but the Kalman filter prevents excitation at higher frequencies.
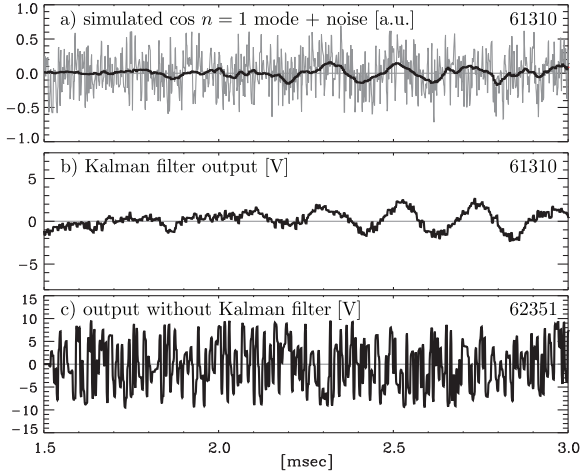
FIG. 4: Adding Gaussian noise to the $n = 1$ mode calculated by the FPGA algorithm showcases the Kalman filter's noise removal capability. Plot a) shows a simulation of the $n = 1$ cosine mode as calculated in the DFT step in the algorithm (black) summed with the Gaussian noise (gray). Plots b) and c) show one of five FPGA outputs to the control coils in the added noise experiments for algorithms with and without the Kalman filter, phased to excite the mode.
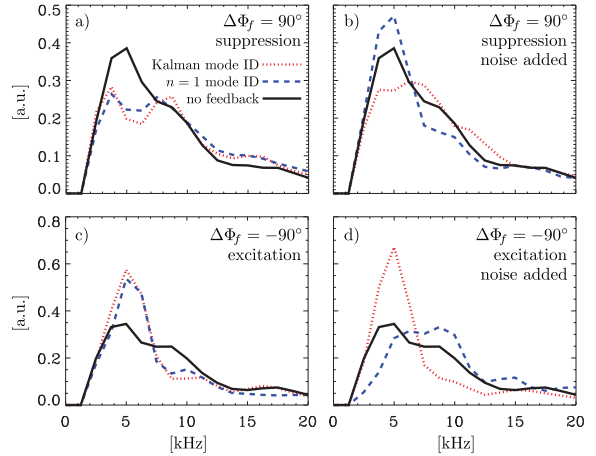
FIG. 5: A comparison of the frequency spectrum of the poloidal field for added noise experiments, for feedback off (solid), Kalman filter mode ID feedback (dotted), and $n = 1$ mode ID feedback (dashed) discharges. Plots a) and c) show suppression and excitation experiments with no added noise. Plots b) and d) show the suppression and excitation cases with extra noise added to the feedback algorithms. With the added noise, the algorithm without the Kalman filter loses its ability to suppress and excite the mode, while the Kalman filter algorithm does not.

In order to demonstrate the Kalman filter's ability to produce reliable estimates of the modes amplitude and phase with noisy inputs, additional noise was mixed with the sensor coil measurements in the feedback algorithm. The noise had an approximately Gaussian probability distribution with zero mean and a flat frequency spectrum. It was introduced after the Discrete Fourier Transform DFT stage in the algorithm, effectively adding a random amplitude and phase to the measured $n = 1$ mode. The amplitude of the added noise was chosen so that its RMS level was close to that of the signals from the sensor coils. Fig. 3. shows a calculation of the cosine component of the $n = 1$ mode with the added noise and example output from the feedback algorithm with and without the Kalman filter. When the Kalman filter is absent from the feedback algorithm, the spatial and temporal filters remain; this case is referred to as "$n = 1$ mode ID." Fig. 5 shows the shot-averaged frequency response in the sensor coils for the Kalman filter and $n = 1$ mode ID algorithms with and without any added noise. Without any extra noise, the performance of both filters in exciting and suppressing fluctuations near 5 kHz is comparable. When the noise is added, however, the Kalman filter algorithm retains its ability to excite and suppress the mode, while the $n = 1$ mode ID algorithm does not.

In summary, suppression and excitation of the external kink mode using a Kalman filter has been demonstrated. The Kalman filter estimates the amplitude and phase of an $n = 1$ instability using a simple model of a growing, rotating mode. Using the Kalman filter prevents excitation at frequencies higher than that of the unstable mode, and the ability of the Kalman filter algorithm to suppress and excite the mode is not affected by presence of noise at amplitudes that disrupt proportional gain only feedback.

4   Optimal Controller Design for Kink Mode Feedback

While theory, modeling, and experiments have established the effectiveness of magnetic control coils for wall mode feedback stabilization, and recent HBT-EP experiments have demonstrated the usefulness of Kalman filtering in suppressing the RWM in the presence of noise [1], the optimization of these systems to enhance plasma performance further while minimizing feedback power requirements is an ongoing challenge. One path to further enhancement of control system performance is via the use of so-called optimal control theory. Optimal control theory calculation of the feedback gain of the system in addition to the use of Kalman filtering for state estimation can lead to improved system performance over simple proportional-derivative (PD) feedback schemes. In addition, the simple system model of a growing, rotating kink mode used in the HBT-EP Kalman filter experiments can be further refined to include a more exact physics model of the plasma-wall-control coil system leading to better state estimation and hence improved feedback performance.

To date, optimal control theory has been applied to the RWM stabilization problem in DIII-D [13, 14]. There a simple analytic model of the plasma, wall, sensor and feedback coil system was used to describe the system state-space of the DIII-D tokamak similar to that used in the HBT-EP Kalman filtering experiments [1]. The stabilized fluctuation and control signal level are found to be of the order of the noise level in steady state. The approach taken here [2] differs in that it starts with the high dimensional intrinsic state-space structure of the VALEN circuit equations [15] and using standard model reduction techniques derives a quantitative low order model using a balanced realization [16] and matched dc gain truncation. An optimal observer is then designed in the form of a Kalman filter. The Kalman state estimate output is used as the feedback signal to the controller. Optimal control theory is then used to calculate controller parameters that simultaneously minimize a cost functional that is quadratic in the control coil currents and voltages. The optimal observer and controller are both designed in the presence of sensor white noise. Model reduction, in this context, attempts to preserve the relevant dynamic and stability properties of the full model state-space system in a useful low dimensional state approximation. This is important and useful, in that typical controller design complexity is of similar order to the size of the model used to describe the system, and for real-time numerical controller design small order models are required for practical implementation. Note that the HBT-EP Kalman filter described above was a very simple 2×2 matrix system with essentially two modes. Using these techniques [2] we have reduced our large finite element VALEN model which typically consists of ~ 3000 eigenmodes down to a minimum of 8 modes using a balanced realization that weights the modes according to their importance to the system input/output map. A matched dc gain truncation is then used to eliminate high frequency modes unnecessary to model the dominant system response poles. An optimal controller and Kalman filter was designed for this reduced, 8 mode model of ITER. The results of using this controller and Kalman filter led to both higher plasma pressure performance and reduction of required control power levels for stabilization to a few megawatts as seen in Fig. 6. The power requirements for stabilization in steady state are based on the assumption that the ITER noise level is 10 G. Sensitivity of the required power to stabilize the RWM to this noise level can simply be scaled as the square of the ratio of the noise amplitudes.

These optimal control and Kalman filtering techniques will have significant benefits if incorporated into the ITER wall mode control system to enhance high beta burning plasma performance. The challenge of finding an appropriate method to reduce the VALEN state-space for the purpose of designing a real-time observer and controller was successfully solved using balanced realization and matched dc gain truncation techniques. An optimal controller and ob-
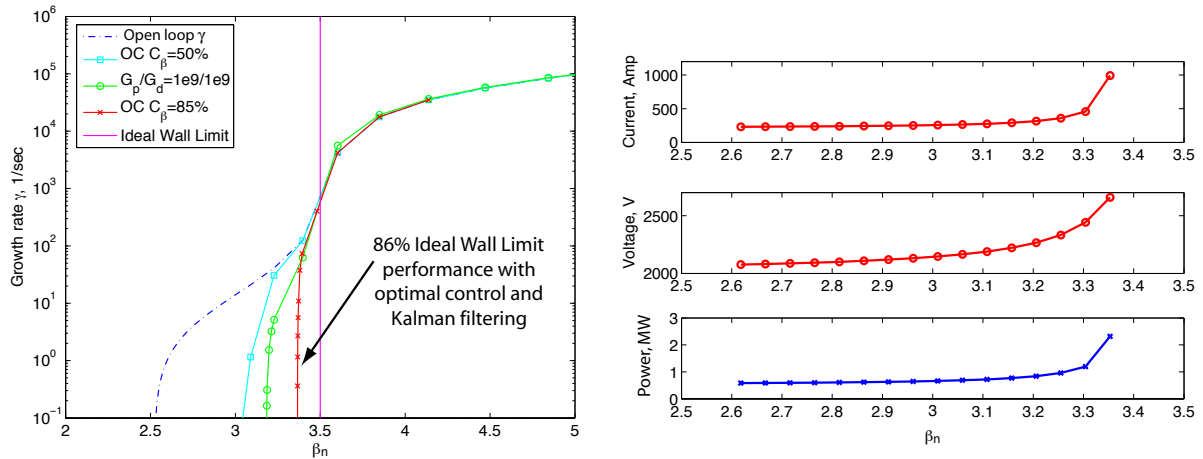
FIG. 6: *(Left) Growth rate, γ, as a function of β_N for feedback calculations using full VALEN model with PD control, reduced order optimal control and the wall mode open loop growth rate [2]. (Right) Control coil current, voltage and power required to stabilize the wall mode as a function of β_N using optimal control. The ideal wall limit of $\beta_N = 3.5$ is calculated for a VALEN model of ITER without blanket modules.*

server designed based on a reduced order VALEN model not only requires considerably less power to operate in steady state with ambient measurement white noise, as was expected, but it also stabilized the RWM for significantly higher plasma pressure values than the classical simple PD type controller. Optimal control offers significant benefits for the control of the RWM and the enhancement of the pressure limits of ITER burning plasmas.

References

[1] J. M. Hanson, B. D. Bono, R. W. James, J. P. Levesque, M. E. Mauel, D. A. Maurer, G. A. Navratil, T. S. Pedersen, and D. Shiraki, *Physics of Plasmas* **15**, 080704 (2008).

[2] O. Katsuro-Hopkins, J. Bialek, D. Maurer, and G. Navratil, *Nuclear Fusion* **47**, 1157 (2007).

[3] A. J. Klein, D. A. Maurer, T. S. Pedersen, M. E. Mauel, G. A. Navratil, C. Cates, M. Shilov, Y. Liu, N. Stillits, and J. Bialek, *Physics of Plasmas* **12**, 040703 (2005).

[4] T. Hender, J. Wesley, J. Bialek, A. Bondeson, A. Boozer, R. Buttery, A. Garofalo, T. Goodman, R. Granetz, Y. Gribov, O. Gruber, M. Gryaznevich, G. Giruzzi, S. Günter, N. Hayashi, P. Helander, C. Hegna, D. Howell, D. Humphreys, G. Huysmans, A. Hyatt, A. Isayama, S. Jardin, Y. Kawano, A. Kellman, C. Kessel, H. Koslowski, R. L. Haye, E. Lazzaro, Y. Liu, V. Lukash, J. Manickam, S. Medvedev, V. Mertens, S. Mirnov, Y. Nakamura, G. Navratil, M. Okabayashi, T. Ozeki, R. Paccagnella, G. Pautasso, F. Porcelli, V. Pustovitov, V. Riccardo, M. Sato, O. Sauter, M. Schaffer, M. Shimada, P. Sonato, E. Strait, M. Sugihara, M. Takechi, A. Turnbull, E. Westerhof, D. Whyte, R. Yoshino, H. Zohm, the ITPA MHD, Disruption, and M. C. T. Group, *Nuclear Fusion* **47**, S128 (2007).

[5] A. M. Garofalo, E. J. Strait, L. C. Johnson, R. J. La Haye, E. A. Lazarus, G. A. Navratil, M. Okabayashi, J. T. Scoville, T. S. Taylor, and A. D. Turnbull, *Phys. Rev. Lett.* **89**, 235001 (2002).

[6] H. Reimerdes, A. M. Garofalo, G. L. Jackson, M. Okabayashi, E. J. Strait, M. S. Chu, Y. In, R. J. L. Haye, M. J. Lanctot, Y. Q. Liu, G. A. Navratil, W. M. Solomon, H. Takahashi, and R. J. Groebner, *Physical Review Letters* **98**, 055001 (2007).

[7] M. Takechi, G. Matsunaga, N. Aiba, T. Fujita, T. Ozeki, Y. Koide, Y. Sakamoto, G. Kurita, A. Isayama, and Y. K. J.-. team, *Physical Review Letters* **98**, 055002 (2007).

[8] C. Cates, M. Shilov, M. E. Mauel, G. A. Navratil, D. Maurer, S. Mukherjee, D. Nadle, J. Bialek, and A. Boozer, *Physics of Plasmas* **7**, 3133 (2000).

[9] M. Okabayashi, J. M. Bialek, M. S. Chance, M. S. Chu, E. D. Fredrickson, A. M. Garofalo, M. Gryaznevich, R. E. Hatcher, T. H. Jensen, L. C. Johnson, R. J. L. Haye, E. A. Lazarus, M. A. Makowski, J. Manickam, G. Navratil, J. T. Scoville, E. J. Strait, A. D. Turnbull, M. L. Walker, and D.-D. Team, *Physics of Plasmas* **8**, 2071 (2001).

[10] S. A. Sabbagh, R. E. Bell, J. E. Menard, D. A. Gates, A. C. Sontag, J. M. Bialek, B. P. LeBlanc, F. M. Levinton, K. Tritz, and H. Yuh, *Physical Review Letters* **97**, 045004 (2006).

[11] M. Mauel, J. Bialek, A. Boozer, C. Cates, R. James, O. Katsuro-Hopkins, A. Klein, Y. Liu, D. Maurer, D. Maslovsky, G. Navratil, T. Pedersen, M. Shilov, and N. Stillits, *Nuclear Fusion* **45**, 285 (2005).

[12] T. S. Pedersen, D. A. Maurer, J. Bialek, O. Katsuro-Hopkins, J. M. Hanson, M. E. Mauel, R. James, A. Klein, Y. Liu, and G. A. Navratil, *Nuclear Fusion* **47**, 1293 (2007).

[13] A. K. Sen, M. Nagashima, and R. W. Longman, *Physics of Plasmas* **10**, 4350 (2003).

[14] Z. Sun, A. K. Sen, and R. W. Longman, *Physics of Plasmas* **13**, 012512 (2006).

[15] J. Bialek, A. H. Boozer, M. E. Mauel, and G. A. Navratil, *Physics of Plasmas* **8**, 2170 (2001).

[16] B. C. Moore, *IEEE Trans. Autom. Control* **AC-26**, 17 (1981).